EFFICIENT TWO-STAGE BEAM TRAINING AND CHANNEL ESTIMATION FOR RIS-AIDED MMWAVE SYSTEMS VIA FAST ALTERNATING LEAST SQUARES

Hyeonjin Chung and Sunwoo Kim

Department of Electronics and Computer Engineering, Hanyang University, Seoul, Korea
Email: {hyeonjingo, remero}@hanyang.ac.kr

ABSTRACT

This paper proposes a two-stage beam training and a channel estimation based on fast alternating least squares (FALS) for reconfigurable intelligent surface (RIS)-aided millimeter-wave systems. To reduce the beam training overhead, only selected columns and rows of the channel matrix are observed by two-stage beam training. This beam training produces a partly observed channel matrix with low coherence, which enables the low rank matrix completion technique to recover unobserved entries. Unobserved entries are recovered by FALS, which alternatingly updates the left and the right singular vectors that comprise the channel. Simulation results and analysis show that the proposed algorithm is computationally efficient and has superior accuracy to existing algorithms.

***Index Terms*—** Reconfigurable intelligent surface, fast alternating least squares, low rank matrix completion, low overhead, channel estimation

1. INTRODUCTION

Recently, a reconfigurable intelligent surface (RIS) is considered as one of key enablers for robust millimeter-wave (mmWave) communications [1]. The RIS can programmably change the propagation characteristics of the signal such as phase and reflection angle [2]. By using this property, the RIS can perform a reflect beamforming to focus the mmWave signal that impinges on the RIS towards the receiver. In this way, the signal can detour the blockage between the transmitter and the receiver. Designing a reflect beamforming vector generally requires the channel estimation [3]. However, the channel estimation for RIS-aided systems suffers from large beam training overhead due to the addition of the RIS between the transmitter and the receiver.

To solve the issue on large beam training overhead, the channel estimation based on compressive sensing (CS) has been proposed in [4–6]. These algorithms exploit CS to estimate the angle-of-departures (AoDs) and the angle-of-arrivals (AoAs) with fewer training signals. Then, they estimate the channel gains to formulate the channel. However, the accuracy of [4–6] is limited by grid-mismatch problem [7]. To enhance accuracy, the channel estimation based on atomic norm minimization (ANM) has been proposed in [8, 9]. Here, the algorithm in [8] exploits the ANM for accurate AoD/AoA estimation while the algorithm in [9] directly estimates the channel by defining appropriate atomic norm. Although the algorithms in [8, 9] are accurate, their computational complexity is excessively high due to Cholesky factorization in semidefinite programming (SDP) [10].

In this paper, we propose the two-stage beam training and the channel estimation based on fast alternating least squares (FALS) [11]. A part of the channel matrix is observed by two-stage beam training, and this partial observation has low coherence. Then, the FALS recovers the unobserved entries, where the number of the unobserved entries is inversely proportional to beam training overhead. Since the FALS is computationally efficient than other low rank matrix completion (LRMC) techniques such as nuclear norm minimization (NNM) [12], the proposed algorithm is both efficient in beam training overhead and computational complexity.

2. SYSTEM MODEL

We consider an uplink RIS-aided mmWave system in Fig. 1. A user equipment (UE) transmits the signal to the RIS, and the RIS bounces back the signal to a base station (BS). Here, all signal paths between the UE and the BS are blocked. The BS and the RIS are equipped with M_{B} and M_{R} antennas respectively. The UE is equipped with a single omnidirectional antenna. Antenna arrays that BS and RIS use are uniform planar arrays (UPAs) with half-wavelength spacing. The BS employs full-complexity hybrid beamforming structure, where the BS is equipped with N_{B} RF chains [13]. Owing to the property of the full-complexity hybrid beamforming, the BS can simultaneously form up to N_{B} beams.

A UE-to-RIS channel and a RIS-to-BS channel are denoted by $\mathbf{h}_{\mathrm{UR}} \in \mathbb{C}^{M_{\mathrm{R}} \times 1}$ and $\mathbf{H}_{\mathrm{RB}} \in \mathbb{C}^{M_{\mathrm{B}} \times M_{\mathrm{R}}}$. Both $\mathbf{h}_{\mathrm{UR}}$ and $\mathbf{H}_{\mathrm{RB}}$ follows Saleh-Valenzuela channel model in [6], which considers both azimuth and elevation. A cascaded effective

This research was supported by the MSIP (Ministry of Science, ICT and Future Planning), Korea, under the ITRC (Information Technology Research Center) support program (IITP-2021-2017-0-01637) supervised by the IITP (Institute for Information & communications Technology Promotion).

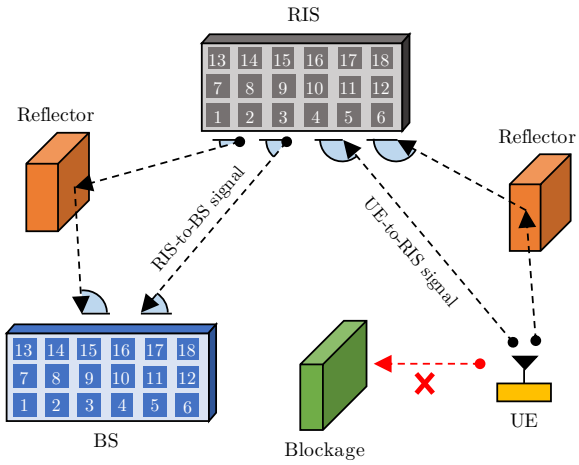

Fig. 1: A scheme of RIS-aided mmWave system. The number on each antenna denotes the index of the antenna. The signal path between BS and UE is blocked.

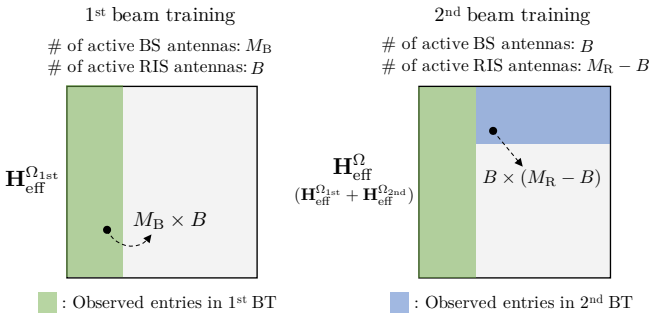

Fig. 2: Observed entries of cascaded effective channel at the first and the second stage beam training.

channel $\mathbf{H}_{\mathrm{eff}} \in \mathbb{C}^{M_{\mathrm{B}} \times M_{\mathrm{R}}}$ is defined as $\mathbf{H}_{\mathrm{RB}}\mathrm{diag}\left(\mathbf{h}_{\mathrm{UR}}\right)$, where $\mathbf{H}_{\mathrm{eff}}$ contains all the channel information.

A RIS control matrix $\boldsymbol{\Omega}$ can be given by

$$\boldsymbol{\Omega} = \begin{bmatrix} \beta_1 e^{j\vartheta_1} & \cdots & 0 & 0 \\ 0 & \beta_2 e^{j\vartheta_2} & \cdots & 0 \\ \vdots & \vdots & \ddots & \vdots \\ 0 & 0 & \cdots & \beta_{M_{\mathrm{R}}} e^{j\vartheta_{M_{\mathrm{R}}}} \end{bmatrix} \in \mathbb{C}^{M_{\mathrm{R}} \times M_{\mathrm{R}}}, \tag{1}$$

where β_m and ϑ_m respectively denote a reflection coefficient and a phase shift of the m-th antenna in the RIS. $\vartheta_m \in [0, 2\pi)$ and β_m can be either 0 or 1, where 0 and 1 respectively denote the deactivation and the activation of the m-th antenna in the RIS. For a convenient representation of $\boldsymbol{\Omega}$, a RIS control vector $\boldsymbol{\omega}$ is defined as

$$\boldsymbol{\omega} = \left[\beta_1 e^{j\vartheta_1}, \beta_2 e^{j\vartheta_2}, \ldots, \beta_{M_{\mathrm{R}}} e^{j\vartheta_{M_{\mathrm{R}}}}\right]^T \in \mathbb{C}^{M_{\mathrm{R}} \times 1}. \tag{2}$$

Note that $\boldsymbol{\Omega} = \mathrm{diag}(\boldsymbol{\omega})$, where $\mathrm{diag}(\cdot)$ denotes the diagonal matrix whose diagonal entries equal to entries of given vector.

3. TWO-STAGE BEAM TRAINING FOR CHANNEL MATRIX OBSERVATION

3.1. First Stage Beam Training: Observing Columns

During the first stage beam training, the BS activates all antennas in the array while the RIS activates B antennas. This leads to observation of B columns of $\mathbf{H}_{\mathrm{eff}}$. At the first stage, the BS employs $M_{\mathrm{B}}/N_{\mathrm{B}}$ combining matrices. The combining matrix changes by each training symbol which is composed of D pilot signal samples. There are B frames, and each frame consists of $M_{\mathrm{B}}/N_{\mathrm{B}}$ training symbols. The RIS control matrix changes frame by frame. This frame structure is equivalent to that of [9].

A procedure of transmitting, receiving, and compiling training symbols also follows that of [9]. A compilation of all the pilot signals received at the first stage, $\mathbf{Y}_{1\mathrm{st}} \in \mathbb{C}^{M_{\mathrm{B}} \times B}$, can be represented as

$$\mathbf{Y}_{1\mathrm{st}} = P_{\mathrm{Tx}} \mathbf{C}_{1\mathrm{st}}^H \mathbf{H}_{\mathrm{eff}} \mathbf{W}_{1\mathrm{st}} + \mathbf{V} \in \mathbb{C}^{M_{\mathrm{B}} \times B}, \tag{3}$$

where P_{Tx} is a transmission power of the UE. $\mathbf{C}_{1\mathrm{st}} \in \mathbb{C}^{M_{\mathrm{B}} \times M_{\mathrm{B}}}$ is a full rank matrix which contains all combining matrices used during the first stage beam training. Generally, $\mathbf{C}_{1\mathrm{st}}$ is set as $M_{\mathrm{B}} \times M_{\mathrm{B}}$ discrete Fourier transform (DFT) matrix [14]. $\mathbf{W}_{1\mathrm{st}} \in \mathbb{C}^{M_{\mathrm{R}} \times B}$ is a matrix which contains all RIS control vectors used during the first stage beam training. $\mathbf{W}_{1\mathrm{st}}$ is set as follows.

$$\mathbf{W}_{1\mathrm{st}} = \left[\boldsymbol{\Psi}_B^T, \mathbf{O}_{B, M_{\mathrm{R}}-B}\right]^T \in \mathbb{C}^{M_{\mathrm{R}} \times B}, \tag{4}$$

where $\boldsymbol{\Psi}_B$ is a $B \times B$ DFT matrix. $\mathbf{O}_{M,N}$ denotes a $M \times N$ zero matrix. $\mathbf{W}_{1\mathrm{st}}$ represents that the RIS exploits B antennas to form B beams. $\mathbf{V}$ is a matrix that represents the noise whose entries all follow $\mathcal{CN}(0, \sigma^2/D)$. Here, σ^2 denote the power of noise.

Entries of $\mathbf{H}_{\mathrm{eff}}$ observed after the first beam training, $\mathbf{H}_{\mathrm{eff}}^{\Omega_{1\mathrm{st}}}$, can be derived as

$$\mathbf{H}_{\mathrm{eff}}^{\Omega_{1\mathrm{st}}} = \frac{\left(\mathbf{C}_{1\mathrm{st}}^H\right)^{-1} \mathbf{Y}_{1\mathrm{st}} \mathbf{W}_{1\mathrm{st}}^H}{B P_{\mathrm{Tx}}} \in \mathbb{C}^{M_{\mathrm{B}} \times M_{\mathrm{R}}}. \tag{5}$$

Fig. 2 shows the observed entries of $\mathbf{H}_{\mathrm{eff}}$. The entries of $\mathbf{H}_{\mathrm{eff}}^{\Omega_{1\mathrm{st}}}$ are filled with zero except first B columns.

3.2. Second Stage Beam Training: Observing Rows

During the second stage beam training, the BS activates B antennas, and the RIS activates $M_{\mathrm{R}} - B$ antennas. Here, B RIS antennas activated at the first stage are deactivated at the second stage. The BS employs B/N_{B} combining matrices.

There are $M_R - B$ frames, and each frame consists of B/N_{B} training symbols.

After following identical procedure in [9], $\mathbf{Y}_{\text{2nd}}$, a compilation of all the pilot signals received at the second stage can be given by

$$\mathbf{Y}_{\text{2nd}} = P_{\text{Tx}}\mathbf{C}_{\text{2nd}}^{H}\mathbf{H}_{\text{eff}}\mathbf{W}_{\text{2nd}} + \mathbf{U} \in \mathbb{C}^{B\times(M_{\text{R}}-B)}. \quad (6)$$

$\mathbf{C}_{\text{2nd}} \in \mathbb{C}^{M_{\text{B}}\times B}$ is a matrix that contains B/N_{B} combining matrices. $\mathbf{C}_{\text{2nd}}$ is set as

$$\mathbf{C}_{\text{2nd}} = \left[\mathbf{\Psi}_{B}^{T}, \mathbf{O}_{B,M_{\text{B}}-B}\right]^{T} \in \mathbb{C}^{M_{\text{B}}\times B}, \quad (7)$$

where $\mathbf{C}_{\text{2nd}}$ represents that the BS forms a total of B receive beams using B antennas. $\mathbf{W}_{\text{2nd}} \in \mathbb{C}^{M_{\text{R}}\times(M_{\text{R}}-B)}$ is a matrix that contains the RIS control vectors used during the second stage. $\mathbf{W}_{\text{2nd}}$ is given by

$$\mathbf{W}_{\text{2nd}} = \left[\mathbf{O}_{(M_{\text{R}}-B),B}, \mathbf{\Psi}_{M_{\text{R}}-B}^{T}\right]^{T} \in \mathbb{C}^{M_{\text{R}}\times(M_{\text{R}}-B)}, \quad (8)$$

where $\mathbf{W}_{\text{2nd}}$ represents that $M_{\text{R}} - B$ reflect beams are formed using $M_{\text{R}} - B$ RIS antennas. $\mathbf{U}$ denotes a noise matrix.

Entries of $\mathbf{H}_{\text{eff}}$ observed after the second beam training, $\mathbf{H}_{\text{eff}}^{\Omega_{\text{2nd}}}$, can be derived as

$$\mathbf{H}_{\text{eff}}^{\Omega_{\text{2nd}}} = \frac{\mathbf{C}_{\text{2nd}}\mathbf{Y}_{\text{2nd}}\mathbf{W}_{\text{2nd}}^{H}}{B(M_{\text{R}}-B)P_{\text{Tx}}} \in \mathbb{C}^{M_{\text{B}}\times M_{\text{R}}}. \quad (9)$$

As in Fig. 2, the entries of $\mathbf{H}_{\text{eff}}^{\Omega_{\text{2nd}}}$ are filled with zero except $B(M_{\text{R}} - B)$ observed entries. An entire observation of $\mathbf{H}_{\text{eff}}$, $\mathbf{H}_{\text{eff}}^{\Omega}$ can be given by

$$\mathbf{H}_{\text{eff}}^{\Omega} = \mathbf{H}_{\text{eff}}^{\Omega_{\text{1st}}} + \mathbf{H}_{\text{eff}}^{\Omega_{\text{2nd}}} \in \mathbb{C}^{M_{\text{B}}\times M_{\text{R}}}. \quad (10)$$

The non-zero entries of $\mathbf{H}_{\text{eff}}^{\Omega}$ do not perfectly match with those of $\mathbf{H}_{\text{eff}}$ due to the noise. As shown in Fig. 2, B columns and B rows are observed when $\mathbf{H}_{\text{eff}}^{\Omega_{\text{1st}}}$ and $\mathbf{H}_{\text{eff}}^{\Omega_{\text{2nd}}}$ are merged together.

4. CHANNEL ESTIMATION VIA FAST ALTERNATING LEAST SQUARES

The FALS is one of accurate and computationally efficient LRMC techniques [11]. However, a performance of LRMC techniques including FALS deteriorates when the coherence of the partial observation is high [15]. The coherence becomes largest if one of the columns or rows remain unobserved in its entirety. In $\mathbf{H}_{\text{eff}}^{\Omega}$, there is no column or row that is completely unobserved. Also, $\mathbf{H}_{\text{eff}}$ is a low rank matrix due to the sparse characteristic of the mmWave [16]. For these reasons, the FALS can successfully recover the unobserved entries of $\mathbf{H}_{\text{eff}}^{\Omega}$.

The FALS requires the rank of $\mathbf{H}_{\text{eff}}$ to recover unobserved entries. Since the mmWave channel is sparse, we assume that B is larger than the rank of $\mathbf{H}_{\text{eff}}$. Then, the rank of $\mathbf{H}_{\text{eff}}$ can be estimated by counting large singular values of $\mathbf{H}_{\text{eff}}^{\Omega_{\text{1st}}}$. Letting σ_1 denotes the largest singular value of $\mathbf{H}_{\text{eff}}^{\Omega_{\text{1st}}}$, the estimated rank of $\mathbf{H}_{\text{eff}}^{\Omega}$, R, is set to the number of the singular values which are larger than $0.05\sigma_1$. Note that this criteria for estimating rank can be changed.

Let $\mathbf{\Omega} \in \mathbb{R}^{M_{\text{B}}\times M_{\text{R}}}$ denotes an indicator matrix which satisfies $\mathbf{H}_{\text{eff}}^{\Omega} \approx \mathbf{\Omega} \circ \mathbf{H}_{\text{eff}}$ and is composed of 0 and 1. Here, $\circ$ denotes Hadamard product. $\bar{\mathbf{\Omega}}$ is a matrix whose elements are bitwise inverse of those of $\mathbf{\Omega}$. Then, a problem that FALS solves can be given by follows [11].

$$\min_{\mathbf{A},\mathbf{B}} \frac{1}{2}\|\mathbf{H}_{\text{eff}}^{\Omega} - \mathbf{\Omega} \circ \left(\mathbf{A}\mathbf{B}^{H}\right)\|_{\text{F}}^{2} + \frac{\lambda}{2}\left(\|\mathbf{A}\|_{\text{F}}^{2} + \|\mathbf{B}\|_{\text{F}}^{2}\right), \quad (11)$$

where $\mathbf{A} \in \mathbb{C}^{M_{\text{B}}\times R}$ and $\mathbf{B} \in \mathbb{C}^{M_{\text{R}}\times R}$ denote the optimization variables. If the FALS converges, $\mathbf{A}$ and $\mathbf{B}$ become the scaled left and right singular vectors of $\mathbf{H}_{\text{eff}}$. λ is a parameter that leverages the trade-off between convergence rate and estimation accuracy. The initial values of $\mathbf{A}$ and $\mathbf{B}$, $\mathbf{A}_{(0)}$ and $\mathbf{B}_{(0)}$, are set as R orthonormal column vectors.

The i-th iteration starts by recovering unobserved entries as follows.

$$\mathbf{S} = \mathbf{H}_{\text{eff}}^{\Omega} + \bar{\mathbf{\Omega}} \circ \left(\mathbf{A}_{(i)}\mathbf{B}_{(i)}^{H}\right), \quad (12)$$

where $\mathbf{A}_{(i)}$ and $\mathbf{B}_{(i)}$ denote $\mathbf{A}$ and $\mathbf{B}$ updated at the $(i-1)$-th iteration. $\mathbf{S}$ denotes the matrix recovered by $\mathbf{A}_{(i)}$ and $\mathbf{B}_{(i)}$. Then, we calculate $\mathbf{A}_{(i+1)}$ that minimizes the objective function. Here, variables except $\mathbf{A}_{(i+1)}$ are considered as constants. $\mathbf{A}_{(i+1)}$ can be given by

$$\mathbf{A}_{(i+1)} = \underset{\mathbf{A}}{\text{argmin}} \frac{1}{2}\|\mathbf{S} - \mathbf{A}\mathbf{B}_{(i)}^{H}\|_{\text{F}}^{2} + \frac{\lambda}{2}\|\mathbf{A}\|_{\text{F}}^{2}. \quad (13)$$

$\mathbf{A}_{(i+1)}$ can be alternatively represented as

$$\mathbf{A}_{(i+1)} = \mathbf{S}\mathbf{B}_{(i)}\left(\mathbf{B}_{(i)}^{H}\mathbf{B}_{(i)} + \lambda\mathbf{I}_{R}\right)^{-1}. \quad (14)$$

With $\mathbf{A}_{(i+1)}$, the unobserved entries are updated as

$$\mathbf{T} = \mathbf{H}_{\text{eff}}^{\Omega} + \bar{\mathbf{\Omega}} \circ \left(\mathbf{A}_{(i+1)}\mathbf{B}_{(i)}^{H}\right), \quad (15)$$

where $\mathbf{T}$ denotes the matrix recovered by $\mathbf{A}_{(i+1)}$ and $\mathbf{B}_{(i)}$. As in (13), $\mathbf{B}_{(i+1)}$ can be given by follows.

$$\mathbf{B}_{(i+1)} = \underset{\mathbf{B}}{\text{argmin}} \frac{1}{2}\|\mathbf{T} - \mathbf{A}_{(i+1)}\mathbf{B}^{H}\|_{\text{F}}^{2} + \frac{\lambda}{2}\|\mathbf{B}\|_{\text{F}}^{2}. \quad (16)$$

$\mathbf{B}_{(i+1)}$ can be alternatively represented as

$$\mathbf{B}_{(i+1)} = \mathbf{T}^{H}\mathbf{A}_{(i+1)}\left(\mathbf{A}_{(i+1)}^{H}\mathbf{A}_{(i+1)} + \lambda\mathbf{I}_{R}\right)^{-1}. \quad (17)$$

The procedure of (12)-(17) is considered as one iteration, and the iteration repeats until convergence.

To decide the convergence, the objective function at the i-th iteration, $L_{(i)}$ is defined as

$$L_{(i)} = \frac{1}{2}\|\mathbf{H}_{\text{eff}}^{\Omega} - \mathbf{\Omega} \circ (\mathbf{A}_{(i)}\mathbf{B}_{(i)}^{H})\|_{\text{F}}^{2} + \frac{\lambda}{2}\left(\|\mathbf{A}_{(i)}\|_{\text{F}}^{2} + \|\mathbf{B}_{(i)}\|_{\text{F}}^{2}\right). \quad (18)$$

If $L_{(i-1)} - L_{(i)} < \epsilon$, we judge that iteration reached convergence. Here, ϵ is a threshold value to decide convergence. After the convergence, $\mathbf{H}_{\text{eff}}$ is estimated as

$$\hat{\mathbf{H}}_{\text{eff}} = \mathbf{H}_{\text{eff}}^{\Omega} + \bar{\mathbf{\Omega}} \circ \left(\mathbf{A}_{(i)} \mathbf{B}_{(i)}^{H} \right), \tag{19}$$

where $\hat{\mathbf{H}}_{\text{eff}}$ denotes the estimate of $\mathbf{H}_{\text{eff}}$.

5. SIMULATION RESULTS AND ANALYSIS

In the simulation, the BS and the RIS are equipped with 8×8 UPAs so that $M_{\text{B}} = M_{\text{R}} = 64$. N_{B} is set to 4. The number of pilot signal samples in one training symbol, D is 100. The noise power is -100 dBm so that $\sigma = 10^{-5}$. λ is set to 0.001. The proposed algorithm is compared with NNM [12], ANM [9], and OMP [5]. Here, the channel estimation via NNM uses $\mathbf{H}_{\text{eff}}^{\mathbf{\Omega}}$ as a partial observation. The channel estimation via ANM and OMP are reformed to fit the system model used in this simulation. For OMP, the angular domain is divided by 1° to set discretized grid.

The BS is located in $[0, 0, 10]$ m, and the RIS is located in $[40, 30, 20]$ m. The UE is randomly located in the area of which the center is $[70, 0, 0]$ m and the radius is 10 m. To model the UE-to-RIS channel and the RIS-to-BS channel, we refer to the 28 GHz statistical channel model in [17]. The diffuse paths are not considered, and the number of the signal paths is randomly set between 1 and 6. The path loss coefficient is 2.1. The phase of the channel gains and all AoDs/AoAs except the AoD/AoA of the LoS path are determined randomly. The normalized mean square error (NMSE) is defined as $\mathbb{E}\left[\|\mathbf{H}_{\text{eff}}^{\Omega} - \hat{\mathbf{H}}_{\text{eff}}^{\Omega}\|_{\text{F}}^2 / \|\mathbf{H}_{\text{eff}}^{\Omega}\|_{\text{F}}^2\right]$. The signal-to-noise ratio (SNR) is defined as $\mathbb{E}\left[10\log(\|\mathbf{\Omega} \circ \mathbf{H}_{\text{eff}}\|_{\text{F}}^2 / D\|\mathbf{\Omega} \circ \mathbf{H}_{\text{eff}} - \mathbf{H}_{\text{eff}}^{\Omega}\|_{\text{F}}^2)\right]$ (dB). For computation, Intel CPU i5-7500 (3.40 GHz) and 16 GB RAM are used.

Fig. 3 shows the NMSE according to number of training symbols. The number of training symbols can be adjusted by B, the number of columns or rows to observe. A total number of training symbols equals to $B(M_{\text{B}} + M_{\text{R}} - B)/N_{\text{B}}$. The proposed algorithm can achieve the lowest NMSE regardless of the number of transmitted training symbols. This shows that the proposed algorithm can accurately estimate the channel even when the beam training overhead is further reduced. The ANM is the second best option, and the estimation of the NNM becomes accurate if more than 800 training symbols are used. The NMSE of the OMP saturates around 0.07 due to the grid-mismatch.

The computational complexity of all algorithms are analyzed in Table 1. η is the number of iterations for FALS, and G is a size of the grid. To compare the computational complexity fairly, R is neglected since it is very small due to the sparse characteristic of mmWave. Then, we can conclude that the ANM is most computationally demanding, and the NNM follows next. Note that both ANM and NNM are

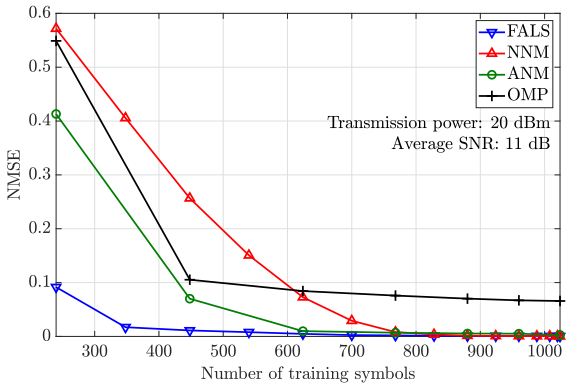

Fig. 3: NMSE according to number of training symbols. The transmission power of the UE is 20 dBm, and the average SNR is 11 dB.

Table 1: Analysis on Computational Complexity

Algorithm	Computational complexity
FALS	$\mathcal{O}\left(\eta\left(M_{\text{B}}M_{\text{R}} + R\left(M_{\text{B}} + M_{\text{R}}\right) + R^2\right)\right)$
NNM [12]	$\mathcal{O}\left(\left(M_{\text{B}} + M_{\text{R}}\right)^{3.5}\right)$
ANM [9]	$\mathcal{O}\left(M_{\text{R}}^4\left(M_{\text{B}} + M_{\text{R}}\right)^{2.5}\right)$
OMP [5]	$\mathcal{O}\left(RM_{\text{B}}BG\right)$

based on SDP. The proposed algorithm is more computationally efficient than ANM and NNM. However, it is difficult to compare the computational complexity between proposed algorithm and OMP based on Table 1. Under current simulation settings, the average computation time of FALS, NNM, ANM, and OMP are 0.27, 7.3, 277, and 0.14 seconds respectively.

6. CONCLUSIONS

In this paper, we propose the two-stage beam training and the channel estimation based on FALS for RIS-aided mmWave systems. To reduce the coherence of the partial observation, the proposed beam training aims to observe columns and rows of the cascaded effective channel matrix. After two-stage beam training, the unobserved entries of the channel are recovered via FALS, which alternatingly updates the left and the right singular vectors that comprise the channel. Simulation results show that the proposed algorithm has superior accuracy to other existing algorithms when using equivalent number of training symbols. Also, the proposed algorithm is computationally more efficient than the algorithms that require SDP.

7. REFERENCES

[1] M. Di Renzo *et al.*, "Smart radio environments empowered by reconfigurable intelligent surfaces: How it works, state of research, and the road ahead," *IEEE J. Sel. Areas Commun.*, vol. 38, pp. 2450–2525, Jul. 2020.

[2] M. A. ElMossallamy *et al.*, "Reconfigurable intelligent surfaces for wireless communications: Principles, challenges, and opportunities," *IEEE Trans. Cogn. Commun. Netw.*, vol. 6, pp. 990–1002, Sep. 2020.

[3] J. Mirza and B. Ali, "Channel estimation method and phase shift design for reconfigurable intelligent surface assisted MIMO networks," *IEEE Trans. Cogn. Commun. Netw.*, vol. 7, pp. 441–451, Apr. 2021.

[4] P. Wang, J. Fang, H. Duan, and H. Li, "Compressed channel estimation for intelligent reflecting surface-assisted millimeter wave systems," *IEEE Signal Process. Lett.*, vol. 27, pp. 905–909, May 2020.

[5] K. Ardah, S. Gherekhloo, A. Andre L. F. de, and M. Haardt, "TRICE: A channel estimation framework for RIS-aided millimeter-wave MIMO systems," *IEEE Signal Process. Lett.*, vol. 28, pp. 513–517, Feb. 2021.

[6] X. Wei, D. Shen, and L. Dai, "Channel estimation for RIS assisted wireless communications—part ii: An improved solution based on double-structured sparsity," *IEEE Commun. Lett.*, vol. 25, pp. 1403–1407, Jan. 2021.

[7] Y. Chi, L. L. Scharf, A. Pezeshki, and A. R. Calderbank, "Sensitivity to basis mismatch in compressed sensing," *IEEE Trans. Signal Process.*, vol. 59, pp. 2182–2195, May 2011.

[8] J. He, H. Wymeersch, and M. Juntti, "Leveraging location information for RIS-aided mmWave MIMO communications," *IEEE Wireless Commun. Lett.*, vol. 10, pp. 1380–1384, Mar. 2021.

[9] H. Chung and S. Kim, "Location-aware channel estimation for RIS-aided mmWave MIMO systems via atomic norm minimization," *arXiv*, Jul. 2021.

[10] R. Madani, A. Kalbat, and J. Lavaei, "A low-complexity parallelizable numerical algorithm for sparse semidefinite programming," *IEEE Trans. Control Netw. Syst.*, vol. 5, pp. 1898–1909, Dec. 2018.

[11] T. Hastie, R. Mazumder, J. D. Lee, and R. Zadeh, "Matrix completion and low-rank SVD via fast alternating least squares," *J. Mach. Learn. Res.*, vol. 16, pp. 3367–3402, Dec. 2015.

[12] E. J. Candès and B. Recht, "Exact matrix completion via convex optimization," *Found. Comput. Math.*, vol. 9, pp. 717–772, Apr. 2009.

[13] A. F. Molisch *et al.*, "Hybrid beamforming for massive MIMO: A survey," *IEEE Commun. Mag.*, vol. 55, pp. 134–141, Sep. 2017.

[14] A. Sayeed and N. Behdad, "Continuous aperture phased MIMO: Basic theory and applications," in *2010 48th Annu. Allerton Conf. Commun., Control, Comput. (Allerton)*, pp. 1196–1203, Oct. 2010.

[15] L. T. Nguyen, J. Kim, and B. Shim, "Low-rank matrix completion: A contemporary survey," *IEEE Access*, vol. 7, pp. 94215–94237, Jul. 2019.

[16] O. E. Ayach, S. Rajagopal, S. Abu-Surra, Z. Pi, and R. W. Heath, "Spatially sparse precoding in millimeter wave MIMO systems," *IEEE Trans. Wireless Commun.*, vol. 13, pp. 1499–1513, Mar. 2014.

[17] M. K. Samimi and T. S. Rappaport, "3-D millimeter-wave statistical channel model for 5G wireless system design," *IEEE Trans. Microw. Theory Tech.*, vol. 64, pp. 2207–2225, Jun. 2016.